Paper396

Soft Matter

PAPER

View Article Online
View Journal | View Issue

CrossMark click for updates

Cite this: *Soft Matter*, 2016, 12, 246

A soft biomolecule actuator based on a highly functionalized bacterial cellulose nano-fiber network with carboxylic acid groups

Fan Wang,†[a] Jin-Han Jeon,†[b] Sukho Park,*[a] Chang-Doo Kee,[a] Seong-Jun Kim[c] and Il-Kwon Oh*[b]

Received 25th March 2015,
Accepted 26th September 2015

DOI: 10.1039/c5sm00707k

www.rsc.org/softmatter

Upcoming human-related applications such as soft wearable electronics, flexible haptic systems, and active bio-medical devices will require bio-friendly actuating materials. Here, we report a soft biomolecule actuator based on carboxylated bacterial cellulose (CBC), ionic liquid (IL), and poly (3,4-ethylenedioxythiophene)–poly(styrenesulfonate) (PEDOT:PSS) electrodes. Soft and biocompatible polymer–IL composites were prepared *via* doping of CBC with ILs. The highly conductive PEDOT:PSS layers were deposited on both sides of the CBC–IL membranes by a dip-coating technique to yield a sandwiched actuator system. Ionic conductivity and ionic exchange capacity of the CBC membrane can be increased up to 22.8 times and 1.5 times compared with pristine bacterial cellulose (BC), respectively, resulting in 8 times large bending deformation than the pure BC actuators with metallic electrodes in an open air environment. The developed CBC–IL actuators show significant progress in the development of biocompatible and soft actuating materials with quick response, low operating voltage and comparatively large bending deformation.

Published on 28 September 2015. Downloaded on 17/12/2015 05:49:50.

Introduction

Electroactive polymers (EAPs) that exhibit large bending deformation in response to electrical stimulation have been called "artificial muscles" and have received great attention in recent years due to their biomimetic actuation, large bending deformation, flexibility, light weight, and relatively low-cost.[1] These characteristics make EAPs attractive candidates for various applications to mobile flexible displays, wearable electronics, soft haptic devices, smart electronics textiles, biomimetic sensory-actuators, and biomedical devices.[2–7] Among EAPs, ionic polymer actuators working in open air without solution environmental assistance have been investigated and developed in the form of conjugated polymers, ionic polymer–metal composites, and carbon nanotubes.[8–10] A typical ionic polymer actuator is composed of one ionic-conductive electrolyte membrane deposited by two electric-conductive electrode films. The bending actuation mechanism of ionic polymer actuators can be attributed to expansion and contraction of the ionic polymer core layer near electrodes induced by the migration of ions under applied voltages. The actuation performance is mainly determined by the electro-chemo-mechanical properties of both the electrolyte and electrode materials. Traditionally, the noble metallic materials such as gold, platinum, and silver are utilized as electrode materials.[11] The existing metallic electrodes and preparation methods have serious drawbacks such as cracking of metal electrodes, low stretchability, time-consuming processes, degradation of the polymer electrolyte, the lack of reproducibility, environmental unfriendliness, and high cost.[12] Also, these metallic electrode materials are limited resources and very expensive for practical applications.

Recently, great attention has been paid to non-metallic, compliant and highly conductive electrodes such as poly(3,4-ethylenedioxythiophene)–poly(styrenesulfonate) (PEDOT:PSS) for soft electroactive polymer actuators.[13–15] Oh *et al.*[16] have fabricated a high-performance ionic polymer actuator showing large bending deformation, which is attributed to the synergistic effects of the ion migration of the dissociated ionic liquids inside the membrane and the electrochemical doping processes of the PEDOT:PSS electrodes. Thus far, the highly conductive PEDOT:PSS materials can be a strong candidate for the soft and flexible electrodes of ionic polymer actuators.

For last two decades, ionic polymer actuators have been extensively investigated and greatly improved to satisfy the desired requirements of practical engineering applications. In particular, some human-related applications including smart

[a] *School of Mechanical Engineering, Chonnam National University, 77 Yongbong-ro, Buk-gu, Gwangju 500-757, Republic of Korea. E-mail: spark@jnu.ac.kr*
[b] *Department of Mechanical Engineering, Korea Advanced Institute of Science and Technology, 291 Daehak-ro, Yuseong-gu, Daejeon 305-701, Republic of Korea. E-mail: ikoh@kaist.ac.kr*
[c] *Dept. of Environmental Engineering, Chonnam National University, 77 Yongbong-ro, Buk-gu, Gwangju 500-757, Republic of Korea*
† These authors equally contributed to this work.

This journal is © The Royal Society of Chemistry 2016

Published on 28 September 2015. Downloaded on 17/12/2015 05:49:50.

electronic textiles, wearable soft electronics, soft haptic electronics, and disposable active bio-medical devices will require high performance soft actuators with bio-friendly, biocompatible, and biodegradable functionalities. A promising way to meet these requirements is to use naturally abundant biopolymers such as plant cellulose, cellulose acetate, chitosan, and bacterial cellulose, which are light weight, low-cost, and sustainable resources. However, conventional biopolymer actuators still have relatively low actuation performance due to the low electro-chemo-mechanical properties.

Among electroactive biopolymers, bacterial cellulose (BC) is an interesting biological material produced by several different types of bacteria.[17] Quite different from plant cellulose and *Cladophora* cellulose, BC has more crystalline and porous, higher water uptake capacity, higher ionic exchange capacity, and no lignin or hemicellulose in comparison with plant cellulose. Particularly, BC is essentially an assembly of cellulose microfibrils based on van der Waals and hydrogen bonding interactions within and between bacterial cellulose molecules because of the presence of many –OH radicals on the bacterial cellulose chains, which cause the fibers to entangle together tightly and therefore form an insoluble compound. Our group recently developed a bacterial cellulose actuator which could be electrically activated under fully hydrated conditions,[18] but it showed low bending deformation and poor durability resulting from an aggregated and entangled BC fiber matrix. Until now, BC-based artificial muscles show relatively low ionic exchange capacity, low ionic conductivity, high mechanical stiffness, and low actuation performance compared with other synthetic ionic polymer actuators.

Recently, many researchers have successfully fabricated BC micro-fibril dispersions by the chemical treatment of the original conventional gel-type bacterial cellulose using the 2,2,6,6-tetramethylpylperidine-1-oxyl (TEMPO)-mediated oxidation method.[19,20] The TEMPO-oxidized bacterial cellulose nanofibrils with uniform widths of 3–6 nm possess superior physical properties such as a high aspect ratio, a high surface-to-volume ratio, low thermal expansion, and high elastic properties.[21] Without significant changes to the crystallinity of BC, C6 carboxylate (COO^-H^+) moieties are selectively oxidized on each BC microfibril surface, which allow the homogeneous dispersion of completely individual crystalline bacterial cellulose in water due to the electrostatic repulsion between the negatively charged carboxylate ions.[22] Most interestingly, carboxylic acid groups in TEMPO-oxidized bacterial cellulose can be used as protonation-active sites in the bacterial cellulose matrix and can greatly contribute to the absorption of ionic liquid and the enhancement of ion transport properties including an electrochemical activity and outstanding electro-chemo-mechanical properties. Due to the introduction of carboxylate groups on the surface of bacterial cellulose, the TEMPO-oxidized bacterial cellulose can be a porous nano-fiber networked membrane, so called carboxylated bacterial cellulose (CBC). Moreover, CBC can be dispersed in water in the form of one-chain sequences such that more uniform membranes can be easily obtained through a simple casting method. These properties of CBC offer great potential in the field of transparent and flexible films,[20] gas-barrier films,[23] highly active nano-hybrid catalysts,[24] and biomimetic tissue engineering scaffolds.[25] However, there is no report on the use of CBC membranes for soft electroactive biomolecule actuators.

In this study, we newly designed a high-performance soft biomolecule actuator based on CBC, PEDOT:PSS electrodes, and ionic liquid (IL). The CBC–IL actuator under both step and harmonic electrical inputs showed large bending deformation, which could be attributed to its higher ionic exchange capacity, ionic conductivity and tuned mechanical properties, all of which result from the strong ionic interaction between the carboxylic acid groups of CBC and ionic liquid. In addition, another reason for the enhanced performance was due to the synergistic effects of ion migration of ionic liquid inside CBC and the electrochemical doping processes of the PEODT:PSS electrodes.

Experimental section

Materials

2,2,6,6-Tetramethylpylperidine-1-oxy radical (TEMPO, 99%), 12% sodium hypochlorite solution (NaClO, 99%), and sodium bromide (NaBr, 99%) were purchased from Wako Pure Chemical, Japan. 1-Ethyl-3-methylimidazolium tetrafluoroborate ($EMIMBF_4$), sodium hydroxide (NaOH) and hydrochloric acid (HCl) were purchased from Sigma Aldrich. The conducting polymer poly (3,4-ethylenedioxythiophene)–polystyrenesulfonic acid (PEDOT:PSS) is commercially available in the form of a water dispersion (1.3 wt% dispersion in water, Baytron P AG, H. C. Starck). All the chemical reagents are used as received without further purification.

Preparation of BC and CBC

The preparation procedure of BC was described in our previous work.[18] Briefly, BC was cultivated using the Acetobacter Xylinum KJ1 and Glu-Fruc medium, which were used as the BC producer and producer medium, respectively. After incubating 10 days and being statically cultured at 30 °C, the BC obtained from BC production culture was then treated with 0.1 M of the NaOH solution for 20 min to lyse the bacteria and washed with deionized water several times. Carboxylated bacterial cellulose (CBC) was prepared by the TEMPO-mediated oxidation system.[20] 1 g BC was suspended in 100 ml deionized water using a homogenizer (Physcotron NS-56, Microtec). TEMPO (0.016 g, 0.1mmol), NaBr (0.1 g, 1 mmol) and the 12% NaClO solution (3.1 g, 5.0 mmol) were added to the resulting solution. The pH value was maintained at 10.5 by adding NaOH solution (0.5 M). At the end of a predetermined reaction time, the pH was adjusted to 7 by adding HCl (0.5 M). The CBC was then filtered and washed with distilled water several times. Finally, CBC dispersion was obtained by adding 0.5 g CBC to the deionized water (100 ml) under gentle agitation.

Preparation of a CBC–IL membrane

A CBC–IL membrane was prepared by using a solution casting method. Ionic liquid ($EMIMBF_4$) was added into 60 ml CBC dispersion (5 mg/10 ml) at a weight percentage of 0.5%. The mixture was continuously stirred until it became stable dispersion at

Published on 28 September 2015. Downloaded on 17/12/2015 05:49:50.

room temperature for 3 h. After removing the bubbles under vacuum, the stabilized dispersion was poured into a casting device and dried for 10 h at 65 °C in the vacuum oven. The bacterial cellulose nano-fiber networked membrane is finally obtained. In addition, a BC–IL membrane was fabricated using the same process.

Preparation of a CBC–IL actuator

A soft CBC–IL actuator was fabricated by depositing the PEDOT:PSS conducting layers on both sides of the composite membrane *via* a dip-coating method. The composite membrane was dipped into the PEDOT:PSS solution for 5 min and dried sufficiently for 2 h at room temperature. Finally, the soft CBC–IL actuator was obtained and cut with dimensions of 5 mm × 40 mm × 0.08 mm. The schematic illustration of the preparation of a CBC–IL actuator was shown in Scheme 1.

Characterization of membranes

FT-IR, SEM and XRD analysis: the FT-IR spectra of the BC, CBC, and CBC–IL membranes were measured using a FT-IR spectrometer (Spectrum 400, PerkinElmer Co.). The field emission scanning electron microscope (FE-SEM) observations of membranes were taken using a JSM-7500F (JEOL Co.), 3.0 kV microscope. Before capturing the images, the membranes were thoroughly dried, and the surface morphology was investigated. X-ray diffraction (XRD) of the membranes was characterized using a high resolution X-ray diffractometer (X'Pert PRO multipurpose X-ray diffractometer, PANalytical Co.) in the range of 5 to 40°.

Tensile test. The tensile strength properties of the BC, CBC and CBC–IL membranes were carried out using a testing machine (AGS-X+250, Shimadzu Crop., Japan.), which was equipped with a 200 N load cell. The test speed was set to a rate of 10 mm min^{-1}. The cross-sectional area of the samples was tested and the gauge length between the grips was 10 mm. All the membrane samples had a rectangle shape.

Thermogravimetric analysis (TGA). Thermal analysis of the membranes was performed using a Thermogravimetric Analyzer (TGA-50H). All measurements were carried out under nitrogen gas flushed at a flow rate of 50 ml min^{-1}. TGA measurements were done under a nitrogen atmosphere at a heating rate of 10 °C min^{-1} from 40 and 600 °C.

Electrochemical properties. Ionic Exchange Capacity (IEC) indicates the number of mill equivalents of ions in 1.0 g of the dry BC and CBC membranes. The membranes were immersed in a 2 M HCl solution for the ion-exchange of H^+. The acidic form of the membranes was then put in 2 M NaCl solution to exchange the proton ions for sodium ions. Finally, the membranes were washed with deionized water to remove H^+. The IEC (meq g^{-1}) of the membranes was measured from the titration method with 0.01 M NaOH solution using phenolphthalein as an indicator. The IEC can be calculated by using the following equation:

$$\mathrm{IEC} = \frac{\text{Consumed NaOH (ml)} \times \text{molarity of NaOH}}{\text{Weight of the membrane}} \quad (1)$$

Ionic conductivity was determined through the electrochemical impedance spectroscopy (EIS) data obtained from the impedance analyzer (VersaSTAT 3 potentiostat/galvanostat) over the frequency range from 10 MHz to 100 Hz at a voltage of 0.1 V. The membranes 1.0 cm × 1.0 cm and two stainless steel electrodes were set in an ECC-Std electrochemical cell. The distance between the two electrodes was 2.0 cm. The ionic conductivity can be calculated using the following equation:

$$\text{Ionic conductivity} = \frac{1}{R} \times \frac{L\ (\mathrm{cm})}{S\ (\mathrm{cm}^2)} \quad (2)$$

where R is the resistance from the impedance analyzer, and S and L are the area and the thickness of the membranes.

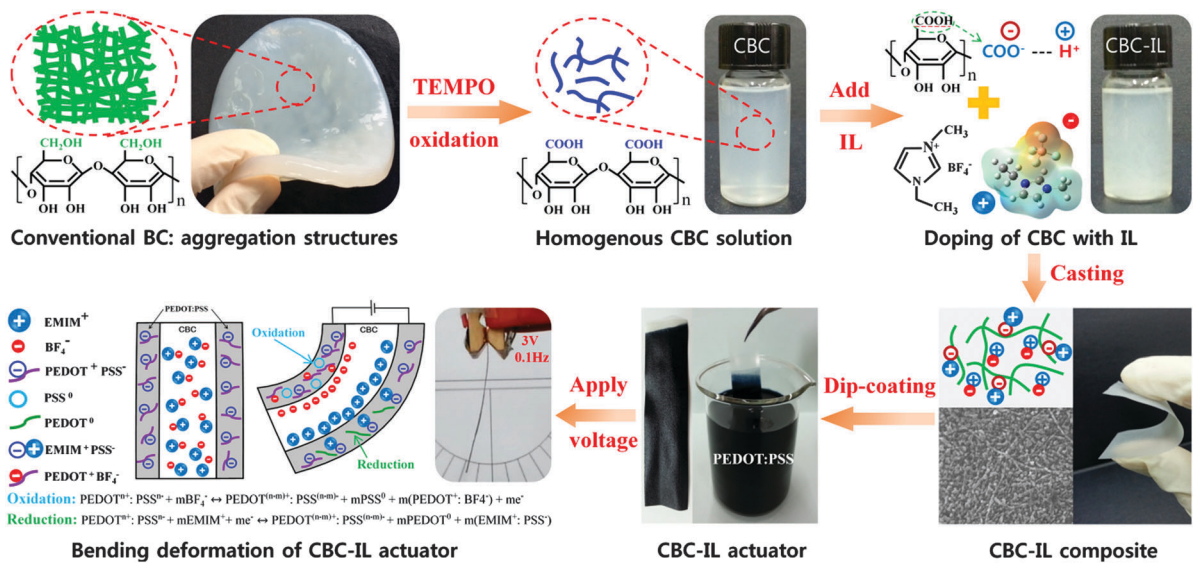

Scheme 1 Schematic illustration of the fabrication and actuation mechanism of soft biomolecule CBC–IL actuator:CBC solution (5 mg/10 ml), IL concentration (0.5 wt%), casting (65 °C, 10 h), dip-coating (5 min) and drying (room temperature).

 This journal is © The Royal Society of Chemistry 2016

Published on 28 September 2015. Downloaded on 17/12/2015 05:49:50.

Setup for actuation tests

The actuator was clamped with about a 5 mm × 4 mm area at one end. For the evaluation of actuation performances, the step response and harmonic response tests were carefully studied.[18] The experimental setup consists of a laser displacement sensor (Keyence-LK031), a current amplifier (UPM1503, Quanser), an NI-PXI 6252 data acquisition board, and an NI-PXI 1409 image acquisition board. All the data acquisition and controls were conducted by an NI-PXI system (1042Q, NI) using a LabVIEW program.

Results and discussion

FT-IR

Fig. 1a shows the FT-IR spectra of the BC, CBC and CBC–IL membranes, which confirm the strong ionic interaction between CBC and ionic liquid. In the spectra of BC membranes, the characteristic peaks of BC can be assigned to:[26] 3342 cm^{-1} (O–H stretching), 3244 cm^{-1} (H-bond), 2906 cm^{-1} (CH stretching of CH_2 and CH_3 groups), 1643 cm^{-1} (C=O stretching), 1370.00 cm^{-1} (CH2 symmetric bending) and 1032 cm^{-1} (C–O stretching). In the case of CBC, the 3600–3000 cm^{-1}, 3000–2820 cm^{-1}, and 1175–1000 cm^{-1} bands indicate the O–H stretching vibration, the C–H stretching vibration, and the C–O–C bonding, respectively. In addition, after TEMPO treatment, the characteristic peak of BC shifted from 1643 to 1604 cm^{-1}, indicating the presence of carboxylic acid groups in the bacterial cellulose.[19,27] In particular, the characteristic peak of CBC–IL membranes occurred at the 1611 cm^{-1} band, which confirms the strong ionic interactions between the carboxylic acid groups of the CBC matrix and the ionic liquid as distinctly shown in Fig. 1b. The spectra of CBC–IL membranes displayed at 3164 and 3120 cm^{-1}, and 749 cm^{-1} are attributed to the C–H of imidazole ring stretching vibration and BF_4^- groups of ionic liquid ([EMIM][BF_4]), respectively. Therefore, the FT-IR analyses clearly prove the formation of an ionic membrane with functionalized carboxylic acid groups and ionic interactions of CBC–IL membranes.

FE-SEM

Fig. 1c shows the surface morphologies of BC, CBC and CBC–IL membranes, which confirm the strong ionic interaction between nano-fibrous CBC and ionic liquid ([EMIM][BF_4]). The FE-SEM of BC exhibits an aggregated and entangled BC fiber matrix. The reason is that BC is essentially an assembly of cellulose microfibrils based on van der Waals and hydrogen bonding interactions within and between bacterial cellulose molecules because of the presence of many –OH radicals on the bacterial cellulose chains, resulting in the fibers to entangle together tightly.[28] In the case of CBC, it shows a fibrous network structure of ultrafine individual cellulose microfibrils, which confirms that the dense and entangled BC fibers were converted to individual nanofibers by a TEMPO-mediated oxidation method.[19] The SEM image of the CBC–IL membrane exhibits that the ionic liquid was well anchored on the surface of CBC fibers. Therefore, based on FT-IR

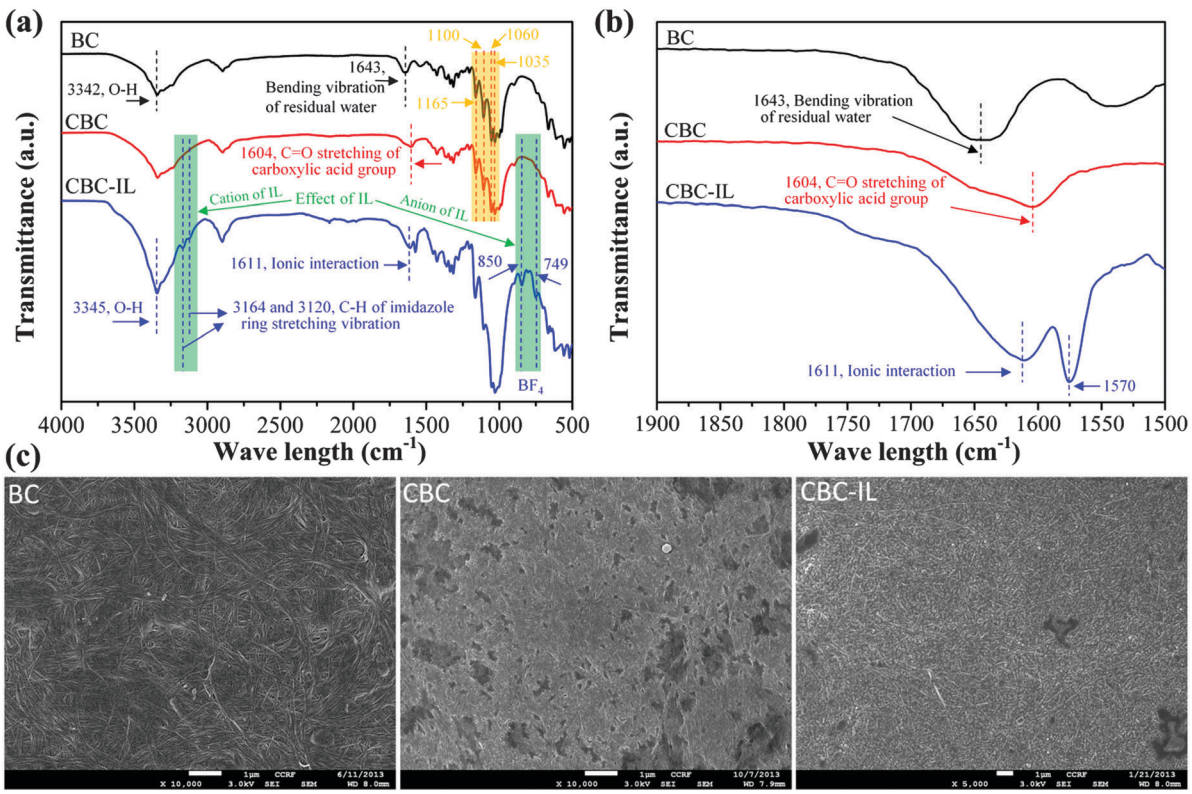

Fig. 1 Chemical analyses and morphological investigations of membranes: (a) FT-IR spectra ranging from 4000 to 500 cm^{-1}, (b) from 1900 to 1500 cm^{-1} of BC, CBC, and CBC–IL, (c) SEM images of BC, CBC, and CBC–IL.

Published on 28 September 2015. Downloaded on 17/12/2015 05:49:50.

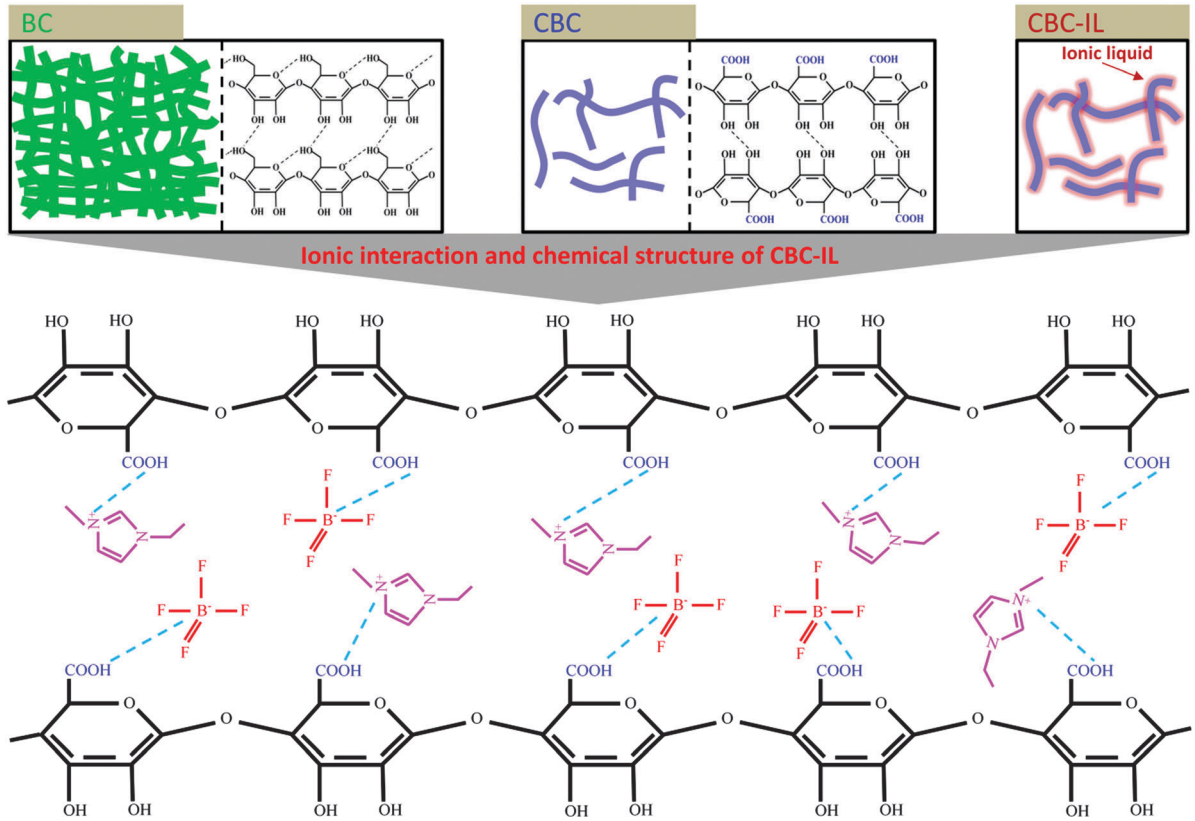

Fig. 2 Chemical structures of BC, CBC and CBC–IL and the corresponding ionic interaction of CBC–IL.

and FE-SEM analyses, the chemical structure of the CBC–IL composite can be described as Fig. 2, which contains the strong ionic interaction occurring between the carboxylic acid groups of CBC and ionic liquid, leading to tuned mechanical stiffness and enhanced interfacial compatibility of the soft CBC–IL composite membrane.

TGA

The thermal properties and stability of CBC–IL composite membranes were investigated by TGA, as shown in Fig. 3a. TGA analysis strongly supports the idea of the ionic interaction of CBC with ionic liquid. The TGA curve of BC having three weight loss steps can be assigned to: the first weight loss (40–130 °C) due to water loss, the second weight loss (300–360 °C) owing to the main chain decomposition and the third weight loss (360–600 °C) attributed to the residual main chain decomposition.[29] For the CBC membrane, the first, second and third weight loss occurred at 40–120 °C, 240–350 °C and 350–600 °C, respectively. It was found that the thermal degradation of CBC started to occur at around 240 °C, while for the original BC, the degradation began at 300 °C. The thermal stability of CBC decreased because of the disruption of the aggregation of the bacterial cellulose matrix and the presence of weakly polar carboxylic acid groups in the CBC matrix.[30] However, with the addition of ionic liquid, the thermal stability of CBC–IL composites was enhanced.

Mechanical properties

The mechanical properties of BC, CBC and CBC–IL membranes are shown in Fig. 3b, and their mechanical properties are compared in Table 1. The tensile modulus decreased from BC to CBC because of the formation of individual bacterial cellulose nanofibrils and the reduction of aggregation and entangled structures. In the case of a CBC–IL membrane, however, the value of tensile strength increased up to 44.26 MPa and it means increase by 12.4% compared with the pure CBC; in particular, the soft CBC–IL composite membrane exhibits an exceptionally superior elongation, up to 22%, which is better than that of BC and CBC membranes. And this reason can be explained with much stronger ionic interaction between ionic liquid and carboxylic acid groups of CBC.

XRD

Fig. 3c shows the variation of crystallinity due to X-ray diffraction of the BC, CBC and CBC–IL membranes. Diffraction peaks of BC at $2\theta = 14.58^\circ$, 16.79° and 22.72° were assigned to the primary diffraction of the $(1\bar{1}0)$, (110) and (220) planes of polymorph cellulose I.[29] For the CBC case, the diffraction peaks displayed at $2\theta = 14.58^\circ$, 17.08° and 22.71°. Moreover, the XRD patterns and crystallinity of CBC are almost the same as those of BC, indicating that BC could be converted to individual nanofibers by TEMPO-mediated oxidation without any significant changes to the original crystallinity or the crystal width of bacterial cellulose.[19,27] In the case of CBC–IL, the diffraction peaks exhibited at $2\theta = 14.58^\circ$, 16.77° and 22.78°. The intensity of peaks at $2\theta = 14.58^\circ$ and 22.78° decreased sharply with the addition of the ionic liquid of [EMIM][BF_4].[31] The crystallinity

 This journal is © The Royal Society of Chemistry 2016

Published on 28 September 2015. Downloaded on 17/12/2015 05:49:50.

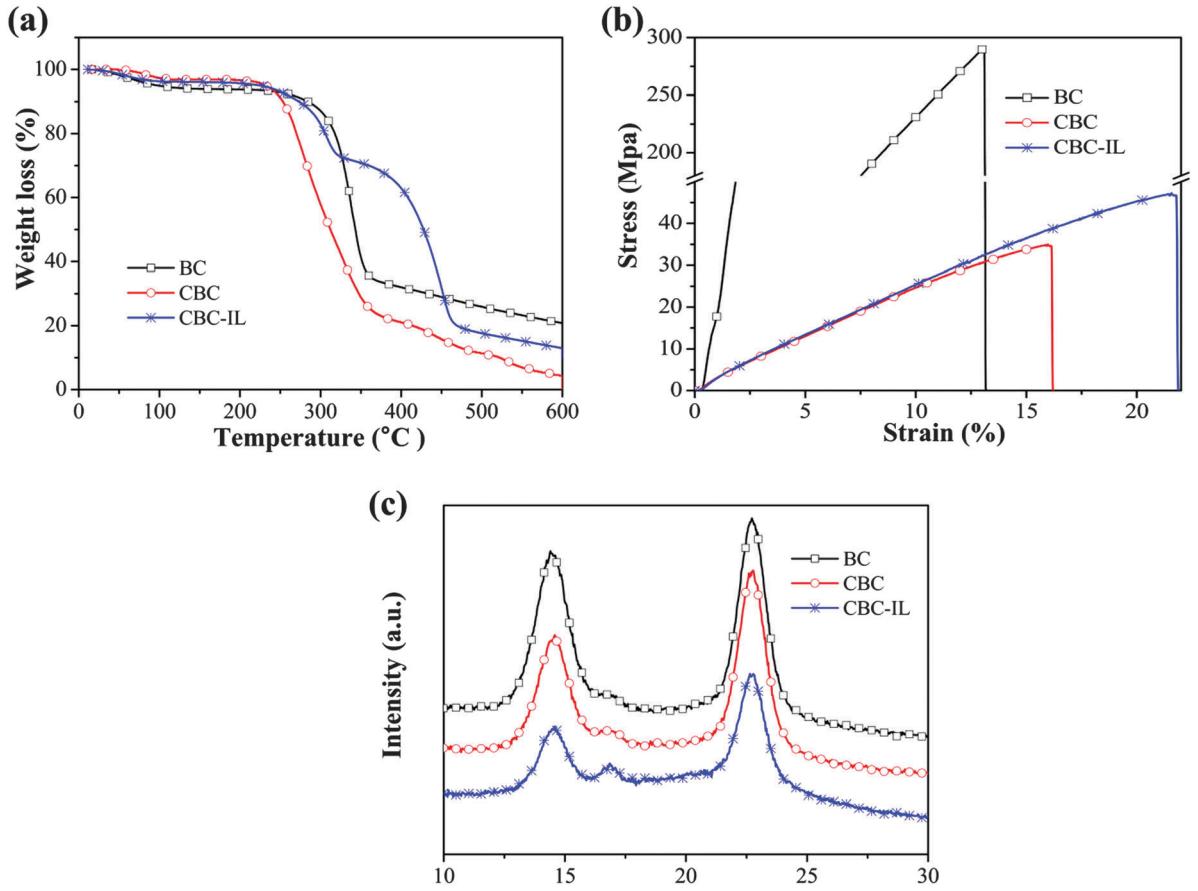

Fig. 3 Thermal and mechanical properties, and X-ray diffraction analyses: (a) TGA, (b) tensile, (c) XRD curves of BC, CBC, and CBC–IL.

Table 1 Mechanical properties of BC, CBC, and CBC–IL

Membrane	Tensile modulus (GPa)	Tensile strength (MPa)	Elonggation (%)
BC	2.91	274.02	12.68
CBC	0.43	39.97	17.53
CBC–IL	0.32	44.26	21.81

index (CI) is used to investigate the changes in the bacterial cellulose structure after the physicochemical and biological treatments based on the following equation:[16]

$$\mathrm{CI} = \frac{I_{\max} - I_{\min}}{I_{\max}} \times 100(\%) \quad (3)$$

where $I_{\max}$ is the maximum intensity between 2θ = 22.7° and 22.9°, $I_{\min}$ is the minimum intensity at 2θ = 18° and 18.2°, which is related to the amorphous region of the bacterial cellulose.[32] The CIs were calculated to be 79.35%, 77.32%, and 38.89%, respectively. This indicates that ionic liquid strongly affects the nanostructure of the CBC networks and that the crystalline region of CBC is transformed into an amorphous region with the addition of ionic liquid, both of which are attributed to the strong ionic interaction between carboxylic acid groups of CBC and ionic liquid, as shown in Fig. 2.

IEC and Ionic conductivity

The ionic exchange capacity (IEC) of the membranes plays a role in evaluating the ionic uptake and ionic conductivity. Table 2 shows the IEC and ionic conductivity values of BC and CBC membranes. The IEC values of the BC and CBC membranes were measured to be 1.10, and 1.82 meq g^{-1}, respectively; the ionic conductivity values of BC and CBC membranes were measured to be 7.9×10^{-5} and 1.8×10^{-3} S cm^{-1}, respectively, which are due to the free availability of carboxylic acid groups of CBC. In addition, the carboxylic acid groups also promote the absorption of ionic liquid. In a word, the high IEC and ionic conductivity of CBC lead to easy ion transport within the membrane under electric stimuli, therefore offering the capability to improve the actuation performances.

Actuation performances

In order to evaluate the soft biomolecule CBC–IL actuator in an open air environment, the step and harmonic electric inputs

Table 2 Electo-chemical properties of BC and CBC

Membrane	IL uptake ratio	IEC (meq g^{-1})	Ionic conductivity (S cm^{-1})
BC	—	1.11	7.9×10^{-5}
CBC	50	1.82	1.8×10^{-3}

Published on 28 September 2015. Downloaded on 17/12/2015 05:49:50.

were applied to the CBC–IL actuator electrodes. Fig. 4a shows the large deformed shapes of soft biomolecule CBC–IL actuators under electrical harmonic input with a 3.0 V peak at 0.1 Hz. Fig. 4b shows the step response of the soft CBC–IL actuator under an applied voltage of 2.5 V direct current (dc). The tip displacement of the CBC–IL actuator is 4.9 mm, while the tip displacements of the previously reported BC actuator[18] and BC–IL actuator are 0.65 mm (having back-relaxation and a long setting time) and 0.97 mm, respectively. The soft biomolecule CBC–IL actuator does not show the back-relaxation which is the main drawback of conventional ionic polymer–metal composite actuators. The reason is attributed to the weakly polar carboxylic acid groups in the CBC matrix. Fig. 4c shows the harmonic responses of the soft biomolecule CBC–IL actuator under sinusoidal excitation of different driving voltages at 0.1 Hz. It is observed that the tip displacement increases with the increment of driving voltage. Fig. 4d shows a comparison for the harmonic responses of the BC,[18] BC–IL and CBC–IL actuators under a sinusoidal excitation with a peak voltage of 2 V at 0.5 Hz. The tip displacement of three samples is ±0.1, ±0.23 and ±0.8 mm, respectively. In both the step and harmonic response cases, the newly developed CBC–IL actuator exhibits better tip displacement due to the higher IEC, ionic conductivity and tuned mechanical properties.

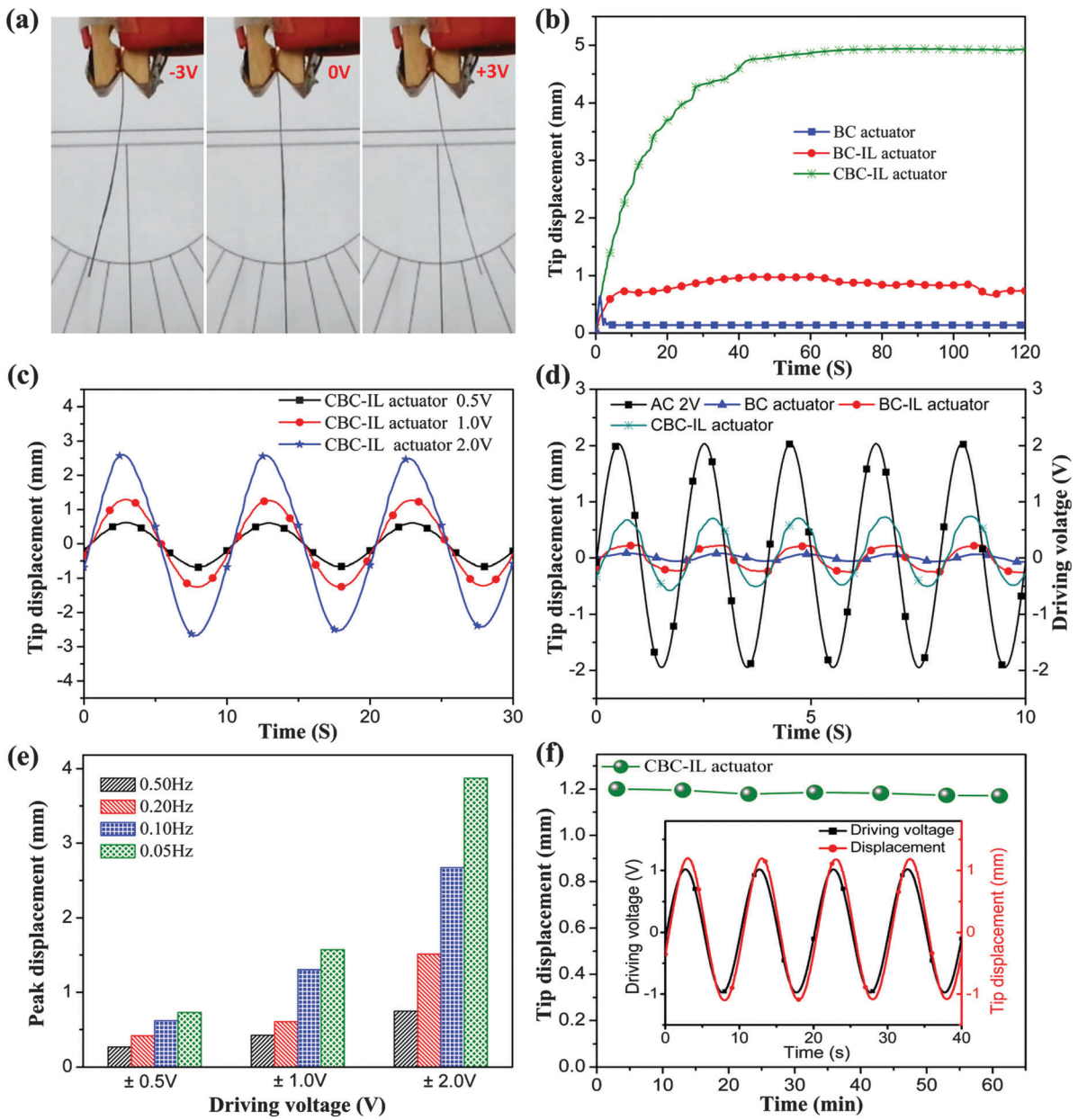

Fig. 4 Actuation performances of soft CBC–IL biomolecule actuators: (a) deformed shapes under sinusoidal excitation of 3 V at 0.1 Hz, (b) step responses under DC 2 V, (c) harmonic responses under different voltages under 0.1 Hz, (d) harmonic responses under 2 V 0.5 Hz, (e) Peak displacements, (f) durability results.

This journal is © The Royal Society of Chemistry 2016

Published on 28 September 2015. Downloaded on 17/12/2015 05:49:50.

Additionally, peak-to-peak displacements were investigated under sinusoidal excitation with ±0.5 to 2.0 V peaks at 0.05, 0.1, 0.2 and 0.5 Hz frequencies, as shown in Fig. 4e. The electrochemical deformation is roughly affected by the driving voltage and applied frequencies because ionic mobility highly depends on the electrical potential field in the polymer matrix. In all tested frequency ranges, the peak tip displacement increases with the increment of the excitation voltage. Most importantly, the soft CBC–IL actuator showed a durable response without significant performance degradation for 60 min under sinusoidal excitation with a 1.0 V peak at 0.1 Hz as shown in Fig. 4f. In addition, the inset of Fig. 4f represents that the actuator still exhibits excellent harmonic responses after a 60 min actuation test without response distortion or performance degradation. This reason is attributed to the synergistic effects of the unique ionic conducting networked matrix and the strong ionic interaction among the ionic liquid, carboxylic acid groups of CBC, and PEDOT:PSS electrodes. The actuation principle of conducting polymers is known as the electrochemical doping process based on the electrochemical redox reaction,[16] as shown in Scheme 1. When the voltage is applied to the PEDOT:PSS electrodes, the layer on the cathode side is oxidized while the other anode layer is reduced. The PEDOT:PSS layer consisting of a p-doped PEDOT-($PEDOT^+$) provides the conducting paths and n-doped PSS^-. Electron transfer into the PEDOT:PSS layer can reduce the $PEDOT^+$ to neutral state ($PEDOT^0$). The ion injection into the PEDOT:PSS layer can oxidize PSS^- to the neutral state (PSS^0). In addition, the molecular size of the cation ($EMIM^+$) is bigger than the anion (BF_4^-). Therefore, the total actuation principle shows the synergistic effects of the ion migration of the ionic liquid of $EMIMBF_4$ inside CBC membranes and the electrochemical doping process of PEDOT:PSS electrodes.

Conclusions

In summary, we report a novel soft biomolecule actuator based on a highly functionalized bacterial cellulose nanofiber network with carboxylic acid groups, PEDOT:PSS conducting polymer electrodes and ionic liquid, resulting in superior electro-chemo-mechanical properties and exceptionally high-performance actuation. The carboxylated bacterial cellulose (CBC) with individual nanofibers and successive mild disintegration was prepared and softened through the TEMPO-oxidation treatment of the bacterial cellulose. The soft CBC–IL membranes were synthesized *via* doping of CBC with ILs, and the PEDOT:PSS layers were deposited on the surfaces of the composites by a dip-coating method. Ionic conductivity and ionic exchange capacity of the CBC membrane can be increased up to 22.8 times and 1.5 times of pristine BC, respectively, resulting in 8 times large bending deformation than the pure bacterial cellulose actuators with metallic electrodes in an open air environment. In addition, the electrochemical doping process of the PEDOT:PSS layers and the ion migration of the dissociated ionic liquid inside CBC due to carboxylic acid groups can be other reasons for the enhanced bending deformation. These synergistic effects are beneficial in making a high performance electroactive actuator which demonstrates improved bending deformation even at the extremely low applied voltage in the open air environment, and the CBC–IL actuator does not show the back-relaxation. Moreover, the developed active materials can be used in human friendly electronics such as soft wearable electronics, flexible haptic systems, and active bio-medical devices.

Acknowledgements

This work was partially supported by the Creative Research Initiative Program (2015R1A3A2028975) funded by National Research Foundation of Korea (NRF) and this work was supported by the NSL (National Space Lab) program through the National Research Foundation of Korea funded by the Ministry of Education, Science and Technology.

Notes and references

1 Y. Osada, H. Okuzaki and H. Hori, *Nature*, 1992, **355**, 242–244.
2 M. Shahinpoor, *Smart Mater. Struct.*, 1992, **1**, 91–94.
3 Y. Bar-Cohen, *Electro Active Polymers (EAP) as artificial Muscles: Reality, Potential, and Challenges*, SPIE Press, Washington USA, 2nd edn, 2001.
4 S. Guo, T. Fukuda and K. Asaka, *IEEE/ASME Trans. Mechatronics*, 2003, **8**, 136–141.
5 K. J. Kim and M. Shahinpoor, *Polymer*, 2002, **43**, 797–802.
6 J. Kim and B. S. Yung, *Smart Mater. Struct.*, 2002, **11**, 355.
7 J. Lu, S. G. Kim, S. Lee and I. K. Oh, *Adv. Funct. Mater.*, 2008, **18**, 1290–1298.
8 J. H. Burroughes, D. D. C. Bradley, A. R. Brown, R. N. Marks, K. Mackay, R. H. Friend, P. L. Burns and A. B. Holmes, *Nature*, 1990, **347**, 539–541.
9 V. Panwar, K. Cha, J. O. Park and S. Park, *Sens. Actuators, B*, 2012, **161**, 460–470.
10 L. Lu and W. Chen, *Adv. Mater.*, 2010, **22**, 3745–3748.
11 J. Li, S. Vadahanambi, C. D. Kee and I. K. Oh, *Biomacromolecules*, 2011, **12**, 2048–2054.
12 R. V. Cheedarala, J. H. Jeon, C. D. Kee and I. K. Oh, *Adv. Funct. Mater.*, 2014, **24**, 6005–6015.
13 F. Greco, A. Zucca, S. Taccola, A. Menciassi, T. Fujie, H. Haniuda, S. Takeoka, P. Dario and V. Mattoli, *Soft Matter*, 2011, **7**, 10642–10650.
14 F. Greco, V. Domenici, A. Desii, E. Sinibaldi, B. Zalar, B. Mazzolai and V. Mattoli, *Soft Matter*, 2013, **9**, 1145–11416.
15 H. Okuzaki, *Sens. Actuators, B*, 2014, **194**, 59–63.
16 S. S. Kim, J. H. Jeon, C. D. Kee and I. K. Oh, *Smart Mater. Struct.*, 2013, **22**, 085026.
17 S. H. Moon, J. M. Park, H. Y. Chun and S. J. Kim, *Biotechnol. Bioprocess Eng.*, 2006, **11**, 26–31.
18 J. H. Jeon, I. K. Oh, C. D. Kee and S. J. Kim, *Sens. Actuators, B*, 2010, **146**, 307–313.
19 A. Isogai, T. Saito and H. Fukuzumi, *Nanoscale*, 2011, **3**, 71–85.
20 F. Wang, S. S. Kim, C. D. Kee, Y. D. Shen and I. K. Oh, *Smart Mater. Struct.*, 2014, **23**, 074006.
21 K. Jradi, B. Bideau, B. Chabot and C. Daneault, *J. Mater. Sci.*, 2012, **47**, 3752–3762.

22 H. Koga, T. Saito, T. Kitaoka, M. Nogi, K. Suganuma and A. Isogai, *Biomacromolecules*, 2013, **14**, 1160–1165.
23 C. N. Wu, T. Saito, S. Fujisawa, H. Fukuzumi and A. Isogai, *Biomacromolecules*, 2012, **13**, 1927–1932.
24 H. Koga, E. Tokunaga, M. Hidaka, Y. Umemura, T. Saito, A. Isogai and T. Kitaoka, *Chem. Commun.*, 2010, **46**, 8567–8569.
25 H. Luo, G. Xiong, D. Hu, K. Ben, F. Yao, Y. Zhu, C. Gao and Y. Wan, *Mater. Chem. Phys.*, 2013, **143**, 373–379.
26 H. S. Barud, R. M. N. Assuncao, M. A. U. Martines, J. Dexpert-Ghys, R. F. C. Marques and S. J. L. Ribeiro, *J. Sol-Gel Sci. Technol.*, 2008, **46**, 363–367.
27 S. lfuku, M. Tsuji, M. Morimoto, H. Saimoto and H. Yano, *Biomacromolecules*, 2009, **10**, 2714–2717.
28 T. Saito, S. Kimura, Y. Nishiyama and A. Isogai, *Biomacromolecules*, 2007, **8**, 2485–2491.
29 K. Qiu and A. N. Netravali, *J. Mater. Sci.*, 2012, **47**, 6066–6075.
30 H. Fukuzumi, T. Saito, Y. Okita and A. Isogai, *Polym. Degrad. Stab.*, 2010, **95**, 1502–1508.
31 S. K. Mahadeva and J. Kim, *J. Phys. Chem. C*, 2009, **113**, 12523–12529.
32 W. Kunchornsup and A. Sirivat, *J. Sol-Gel Sci. Technol.*, 2010, **56**, 19–26.

Published on 28 September 2015. Downloaded on 17/12/2015 05:49:50.

 This journal is © The Royal Society of Chemistry 2016